Journal of Alloys and Compounds 509 (2011) 4731–4737

Contents lists available at ScienceDirect

Journal of Alloys and Compounds

journal homepage: www.elsevier.com/locate/jallcom

Preparation and characterization of barium titanate stannate solid solutions

Nadejda Horchidan[a,*], Adelina C. Ianculescu[b], Lavinia P. Curecheriu[a], Florin Tudorache[a], Valentina Musteata[c], Stefania Stoleriu[b], Nicolae Dragan[d], Dorel Crisan[d], Sorin Tascu[a], Liliana Mitoseriu[a]

[a] Department of Physics, "Al. I. Cuza" University, Bv. Carol 11, Iasi 700506, Romania
[b] Department of Oxide Materials Science and Engineering, Polytechnics University, 1-7 Gh. Polizu, P.O. Box 12-134, 011061 Bucharest, Romania
[c] Institute of Macromolecular Chemistry "Petru Poni", Aleea Grigore Ghica Voda 41A, 700487 Iasi, Romania
[d] Institute of Physical Chemistry "Ilie Murgulescu", Lab. of Oxide Materials Science, 202 Splaiul Independenței, 060021 Bucharest, Romania

ARTICLE INFO

Article history:
Received 18 November 2010
Received in revised form 18 January 2011
Accepted 19 January 2011
Available online 1 February 2011

Keywords:
Barium stannate titanate
Ferroelectrics
Relaxor
Tunability
Hysteresis

ABSTRACT

$BaSn_xTi_{1-x}O_3$ ($x = 0; 0.05; 0.1; 0.15; 0.2$) solid solutions were prepared *via* conventional solid state reaction and sintered at 1300 °C for 4 h, resulting in dense single phase ceramics with homogeneous microstructures. Tetragonal symmetry for $x \leq 0.1$, cubic for $x = 0.2$ and a superposition of tetragonal and cubic for $x = 0.15$ compositions were found by X-ray diffraction analysis. The temperature and frequency dependence of the complex dielectric constant and dc tunability were determined. A transformation from normal ferroelectric to relaxor with diffuse phase transition was observed with increasing the Sn concentration. All the investigated compositions show a relative tunability between 0.55 (for $x = 0.2$) and 0.74 (for $x = 0.1$), at a field amplitude of $E = 20$ kV/cm.

© 2011 Elsevier B.V. All rights reserved.

1. Introduction

Ferroelectric materials are used in many modern technologies such as piezoelectric actuators and electro-optic modulators. One of the most extensively studied perovskite (ABO_3 structure) ferroelectric oxide is barium titanate ($BaTiO_3$), whose excellent dielectric and ferroelectric properties are exploited in various electronic devices as capacitors, thermistors, transducers and nonvolatile memories in microelectronic industry. The properties of barium titanate ceramics are strongly dependent on parameters like: grain size, density, impurities and structural defects [1]. Barium titanate doped with Zr [2], Hf [3], Ce [4], Y [5] and Sn [6] also shows relaxor behavior with improved dielectric performances, very high permittivity, piezoelectric and pyroelectric constants and the lack of macroscopic hysteresis $P(E)$ loop. Complex Pb-based compound oxides, such as $PbMg_{1/3}Nb_{2/3}O_3$ are typical relaxors with excellent dielectric, electromechanic and pyroelectric properties [7], but the disadvantages of their use is related to their complicated formula, large microwave losses, and Pb-based processing causing contamination with Pb, which is a hazardous material. Alternatively, $BaTiO_3$-based solid solutions are environment-friendly dielectrics with performances which tend to be similar as of many Pb-based electroceramics. Therefore, a possible alternatives as relaxors are the heterovalent B-doped $BaTiO_3$ substitutions as $BaZr_xTi_{1-x}O_3$ (BZT), $BaSn_xTi_{1-x}O_3$ (BSnT) and others. At room temperature, the permittivity of BZT is not as high as found in BSnT, which seems a valuable candidate for high permittivity applications. BSnT was also reported as one of the most promising candidates to replace $BaSrTiO_3$ as a microwave dielectric [8]. As in other $BaTiO_3$-based solid solutions, the properties of $BaSn_xTi_{1-x}O_3$ are expected to be tuned by the composition x and by controlling their microstructural characteristics (secondary phases, porosity level, grain size, core–shell structures). The dielectric constant of BSnT solid solution is strongly field-dependent, so that it is possible to control the dielectric constant by adjusting the applied field strength. Based on this property, many devices can be developed such as microwave dielectric amplifiers, parametric devices, frequency multimeters, variable capacitors, phase shifters, tunable filters and voltage controlled oscillators [9], particularly in circuits and devices needed by the wireless communications industry, for scientific, space, commercial and military use.

The solid solution formed by the ferroelectric $BaTiO_3$ and the non-ferroelectric $BaSnO_3$ is one of the earliest prototypes of systems reported to show diffuse ferroelectric–paraelectric phase transition for high Sn additions [7]. Only recently it has aroused highest interest for its abnormal dielectric properties and strong

* Corresponding author. Tel.: +40 232 201102/202405; fax: +40 232 201150.
E-mail address: NHorchidan@stoner.phys.uaic.ro (N. Horchidan).

0925-8388/$ – see front matter © 2011 Elsevier B.V. All rights reserved.
doi:10.1016/j.jallcom.2011.01.123

dielectric nonlinearity [10–13]. As for other $BaTiO_3$-based solid solutions, the Curie temperature and dielectric maximum of the BSnT system can be modified by changing the concentration of Sn. In the last years, Wei and Yao [14], Shvartsman et al. [15], Mueller and Beige [12], Geske et al. [16,17], Wei et al. [18,19] and Cai et al. [20] have studied the dielectric properties, dielectric relaxations, the ferroelectric-relaxor crossover, the diffuse phase transition characteristics, the hysteresis loops under various poling conditions and piezoelectric characteristics of some compositions of BSnT ceramic solid solutions prepared by various methods, while tunability data and relaxor state for high Sn additions $x = 0.20$, 0.30 and 0.40 were also reported in [8]. The large majority of the above mentioned publications do not report composition-dependent structural data. Only Wei and Yao [14] proposed a phase diagram for this system based on the anomalies detected on the dielectric *vs.* temperature dependences, in which a mixture of several structural modifications (rhombohedral, tetragonal and cubic) seems to be present near the room temperatures for the compositions in the range (0.10, 0.15). However, Markovic et al. reported a continuous reducing tetragonality when increasing Sn addition, reaching the value 1 (*i.e.*, cubic structure) for the composition $x = 0.12$ [21]. In spite of various publications concerning the BSnT ceramic system, the succession of its structural phase transitions induced by the Sn addition and a detailed analysis and understanding of the functional properties in direct relationship with the composition, microstructures and phase symmetry is still lacking for this system. In addition, the compositions around $x \sim 0.10$–0.15 are among the most interesting to be still investigated.

In the present paper, we report the results of a systematic study of $BaSn_xTi_{1-x}O_3$ ceramics with compositions $x = 0$, 0.05, 0.1, 0.15 and 0.2 prepared by solid state method, in which the dielectric and tunability properties are investigated and explained in connection with their composition and structural characteristics.

2. Sample preparation and experimental details

$BaSn_xTi_{1-x}O_3$ solid solutions have been prepared by classical ceramic method from p.a. grade oxides and carbonates: TiO_2 (Merck), SnO_2 (Merck) and $BaCO_3$ (Fluka), by a wet homogenization technique in iso-propanol. The initial mixtures were dried and shaped by uniaxial pressing at 160 MPa into pellets of 20 mm diameter and ~3 mm thickness. After the presintering thermal treatment performed in air at 1200 °C with 3 h plateau, the samples were finely grounded in an agate mortar, pressed again into pellets (of 13 mm diameter and ~2 mm thickness) using an organic binder (PVA). These pellets were sintered in air at 1300 °C, with a heating rate of 5 °C/min and a soaking time of 4 h and then they were slowly cooled at the normal cooling rate of the furnace.

X-ray diffraction measurements at room temperature used to investigate the purity of the perovskite phases were performed with a *SHIMADZU XRD 6000* diffractometer using Ni-filtered CuKα radiation ($\lambda = 1.5418$ Å) with a scan step increment of 0.02° and with a counting time of 1 s/step, for 2θ ranged between 20 and 80°. To estimate the structural characteristics, the same step increment, but with a counting time of 10 s/step, for 2θ ranged between 20 and 120° was used. Parameters to define the position, magnitude and shape of the individual peaks were obtained using the pattern fitting and profile analysis of the original X-ray 5.0 program. The lattice constants calculation is based on the least squares procedure (LSP) using the linear multiple regressions for several XRD lines, depending on the unit cell symmetry.

A HITACHI S2600N scanning electron microscope coupled with EDX was used to analyse the microstructure and to check the chemical composition of the ceramic samples.

The electrical measurements were performed on parallel-plate capacitor configuration, by applying Pd–Ag electrodes on the polished surfaces of the sintered ceramic disks. The complex impedance in the frequency range of (1–10^6) Hz was determined by using an impedance analyzer (Solartron, SI 1260). For low temperatures, the complex impedance in the frequency domain (1–10^6 Hz) was determined by using a dielectric spectrometer CONCEPT 40 Novocontrol Tehnologies. The measurements at high voltages were performed by placing the electroded ceramic pellets in a cell containing transformer oil. For obtaining accurate tunability data, a circuit was designed and realized [22], in which the high voltage was obtained from a function generator coupled with a TREK 30/20A-H-CE amplifier.

3. Results and discussion

3.1. Phase purity, structural and microstructural characteristics

For all the investigated ceramics resulted after sintering at 1300 °C/4 h, the room temperature XRD patterns (Fig. 1) show the presence of single-phase perovskite compositions, in the limit of XRD accuracy. The lack of any Ba, Ti or Sn-rich secondary phases demonstrated that, in the mentioned sintering conditions, the solid state reactions, involving the incorporation of the tin additions in the perovskite lattice, were completed.

The results of the calculation of the lattice parameters and unit cell volume of $BaSn_xTi_{1-x}O_3$ ceramics sintered at 1300 °C for 4 h are presented in Table 1. From structural point of view, the $BaSn_xTi_{1-x}O_3$ compositions with lower tin concentration ($x = 0$, 0.05 and 0.10) exhibit at room temperature a tetragonal *P4mm* symmetry of the unit cell. As the tin concentration increases ($x = 0.15$; 0.20), a gradual transition towards a cubic perovskite structure takes place (Table 1). Thus, the composition $x = 0.15$ consists of a mixture of cubic and tetragonal phases, while for the composition with the highest tin concentration ($x = 0.20$) the cubic *Pm3m* symmetry of the unit cell prevails. Consequently, a decrease of the tetragonality degree (expressed as the ratio of the lattice parameters *c* and *a*) was induced by the increase of the tin addition. Since Sn^{4+} incorporated on the titanium sites (octahedral coor-

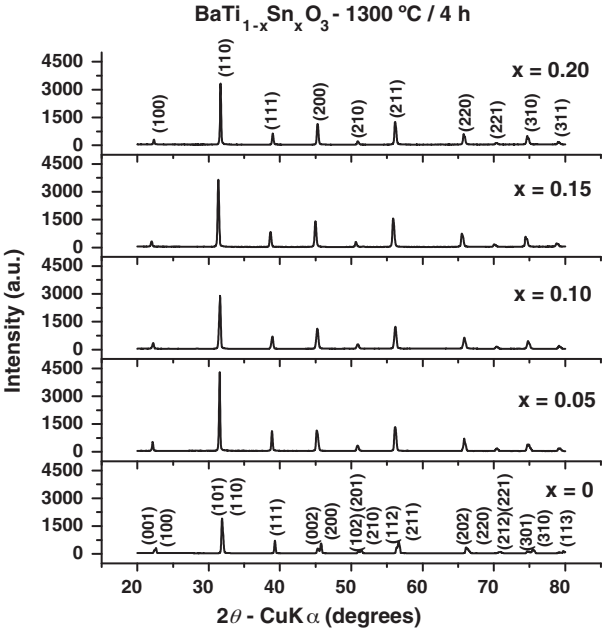

Fig. 1. X-ray diffraction patterns of $BaSn_xTi_{1-x}O_3$ ceramics sintered at 1300 °C for 4 h.

Table 1
Structural parameters of $BaSn_xTi_{1-x}O_3$ ceramics sintered at 1300 °C for 4 h.

Composition, x	Structure	Lattice parameters (Å)		Tetragonality degree, c/a	Unit cell volume, V (Å^3)
		a	c		
0	Tetragonal	3.9713 ± 0.0036	3.9831 ± 0.0047	1.0031 ± 0.0021	62.82 ± 0.19
0.05	Tetragonal	3.9996 ± 0.0003	4.0062 ± 0.0005	1.0017 ± 0.0002	64.09 ± 0.02
0.10	Tetragonal	4.0057 ± 0.0018	4.0127 ± 0.0020	1.0017 ± 0.0009	64.38 ± 0.09
0.15	Cubic	4.0287 ± 0.0009	4.0287 ± 0.0009	1.0000	65.39 ± 0.05
	Tetragonal	4.0165 ± 0.0011	4.0219 ± 0.0016	1.0013 ± 0.0007	64.88 ± 0.06
0.20	Cubic	4.0234 ± 0.0026	4.0234 ± 0.0026	1.0000	65.13 ± 0.13

dination) exhibits a slightly higher value of the ionic radius r (Sn^{4+} = 0.69 Å) than that one corresponding to Ti^{4+} r (Ti^{4+} = 0.67 Å), an expected increase of the lattice parameters and unit cell volume was pointed out (Table 1). Since the presence of orthorhombic phases [17], as well as the superposition of phases with different symmetries [23] was also reported at room temperature for some similar compositions like those ones studied here, calculations for purely orthorhombic phase or for combinations of mixed phases were also carefully performed. The presented data show that only tetragonal and cubic symmetry was identified in the limit of the XRD experiment accuracy. Thus, the present results of the structural calculations are in agreement with the tetragonality reduction reported by Markovic et al. when increasing the Sn addition, for which the cubic structure was reached at the composition x = 0.12 [21].

The surface SEM image for the composition of x = 0.10 (Fig. 2(a)) shows a non-uniform microstructure, with a bimodal grain size distribution. Larger grains (~4.6 μm) coexist with smaller grains (~1.9 μm) and with a certain amount of intergranular pores. Since the coalescence process takes place, the grains present irregular shapes and undefined boundaries, irrespective of their size. All these features demonstrate that, in the mentioned conditions, the sintering process is still in progress. The increase of the tin content to x = 0.20 induces a better densification and tends to inhibit the grain growth (Fig. 2(b)). Therefore, a slight decrease of the overall average grain size can be observed. Even if a slight tendency towards a bimodal grain size distribution still persists, the microstructure seems to be more uniform in this last case.

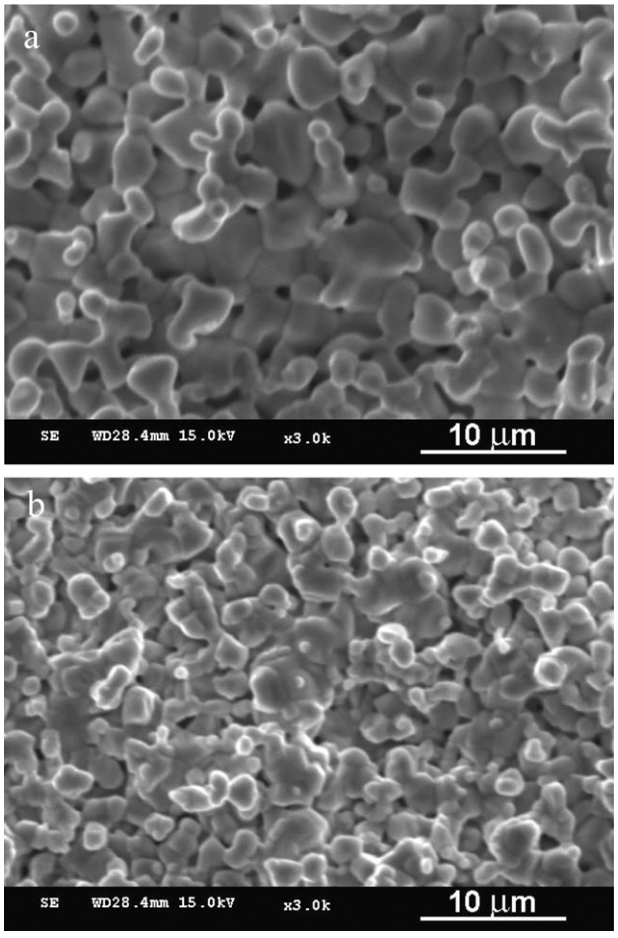

Fig. 2. Surface SEM images of $BaSn_xTi_{1-x}O_3$ ceramics sintered at 1300 °C for 4 h: (a) x = 0.10 and (b) x = 0.20.

3.2. Dielectric spectroscopy characterization

The temperature dependence of the dielectric constant and tangent loss of the BSnT ceramics with different concentrations of Sn (x) at the frequency f = 1 kHz are shown in Fig. 3(a) and (b), respectively. These data revealed high permittivity values over 2000 for the compositions x = 0.05 and x = 0.2, around 4000 for BT and over 5000 for x = 0.1 and x = 0.15 compositions, at room temperature.

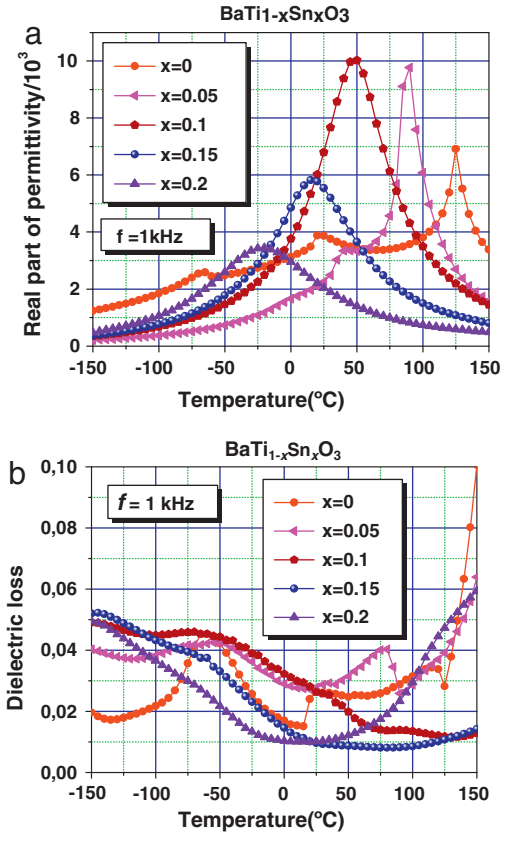

Fig. 3. Temperature dependence of the real part of the dielectric constant (a) and tangent loss tan δ (b) for $BaSn_xTi_{1-x}O_3$ ceramics with different Sn content at the frequency f = 1 kHz.

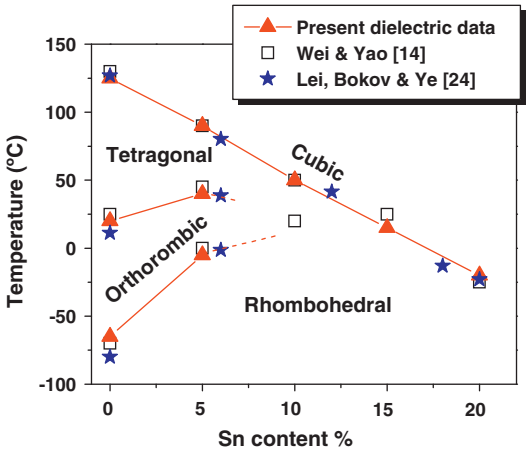

Fig. 4. Phase diagram of BSnT based on the present electrical and XRD data, together with ones proposed by Wei and Yao [14].

Close to room temperature the compositions $x = 0.1$ and $x = 0.15$ show a strong temperature variation of permittivity, induced by the proximity of their ferroelectric–paraelectric phase transitions.

As reported by other authors for similar compositions, the dielectric peaks (and the Curie temperatures T_C) shifts towards lower temperature when increasing the tin concentration (x). Considering that the grain size for all the compositions does not vary significantly (grain size in the range of 1.7–4 μm is typical for all the investigated compositions), the temperature shift can be explained by the structural change from tetragonal towards cubic modifications with increasing the Sn addition, as demonstrated by the XRD analysis and also obtained by other authors [20]. The result is that the phase transition temperature at which the crystalline symmetry of BSnT changes from cubic to tetragonal structure shifts progressively towards a lower temperature when increases Sn addition. For the compositions $x = 0.2$ and $x = 0.15$ the temperature corresponding to the maximum permittivity is below room temperature, which means that BSnT ceramics with tin concentrations above or equal with 0.15 should exhibit a cubic structure at room temperature. For the composition with $x = 0.2$ the results of the electrical measurements showing that at room temperature the system is in its paraelectric state, are again in good agreement with the XRD data, which indicated a fully cubic structure. When the tin content decreases to $x = 0.15$, the coexistence of the cubic and tetragonal modifications determined from the XRD data shows that tetragonal ferroelectric regions still exist slightly above the temperature corresponding to the maximum permittivity T_m. Therefore, at room temperature, the compositions with lower tin content ($x = 0.1$ and $x = 0.05$) exhibiting higher Curie temperatures are in their ferroelectric state, while the other compositions are in the paraelectric cubic state. The results of our electrical measurements (Fig. 4) are in agreement with the data reported by Wei and Yao [14] and Lei et al. [24] for BSnT prepared by solid state reaction from Sn precursors and commercial hydrothermally synthesised $BaTiO_3$ powders.

According to the phase diagram proposed by Wei and Yao [14], a mixture of several modifications (rhombohedral, tetragonal and cubic) might be stabile near the room temperatures for the composition $0.10 < x < 0.15$, as shown in Fig. 4. As mentioned before, other authors reported a continuous reducing tetragonality when increasing the Sn addition and cubic structure for the composition $x = 0.12$ [21] or phase coexistence. In our case, the dielectric data obtained for the concentration $x = 0.05$ revealed another phase transition below 50 °C, attributed to the tetragonal–orthorhombic structural modification, and one near to −5 °C, confirming the fact that at room temperature this composition should have an orthorhombic structure. However, the XRD data indicated for this composition a better fit with only the JCPDS file indexed for a Ba(Sn,Ti)O_3 solid solution (*i.e.*, JCPDS no. 04-007-5135 corresponding to the tetragonal $BaSn_{0.07}Ti_{0.93}O_3$ composition), than any other JCPDS file corresponding to the orthorhombic $BaTiO_3$ state. Therefore, we can conclude, that the orthorhombic distortion in $BaSn_{0.05}Ti_{0.95}O_3$ could be smaller or somewhat different than that one of the orthorhombic state of pure $BaTiO_3$. Taking into account that the calculation of the structural parameters by XRD technique involves an averaging over at least 10^4 unit cells, one can assume that this investigation method is not sensitive enough to make a clear difference between the tetragonal and orthorhombic distortion in the case of the $BaSn_{0.05}Ti_{0.95}O_3$ solid solution and only the electrical measurements against the temperature are able to suggest the presence of the orthorhombic modification. In conclusion, the possible presence of low amounts of other symmetries at room temperature is not excluded for all our compositions $x = 0.05$, 0.10, 0.15 and further detailed experiments allowing a higher local sensitivity (e.g. Raman) are expected to bring more information about the local cation order. For the BSnT ceramic with $x = 0.10$, a difference in the electrical behavior was noticed in our case. Thus, while Wei et al. [18] reported for the $BaTi_{0.9}Sn_{0.1}O_3$ composition two different phase transitions (at 50 °C and at 20 °C, respectively), for our sample with the same Sn content only the higher temperature phase transition at 50 °C was pointed out by the dielectric measurements against the temperature. Our results are in agreement with those of Lei et al. [24], who also found a single phase transition for their $BaTi_{0.9}Sn_{0.1}O_3$ ceramic sample.As reported for other $BaTiO_3$-based solid solutions like BZT [25], a reducing range of temperatures for the stability of the tetragonal state (by reducing the tetragonal–cubic transition temperature T_C and increasing both the rhombohedral–orthorhombic and orthorhombic–tetragonal transition temperatures with different rates) is induced by increasing the homovalent substitutions on the Ti^{4+} sites [14]. As a consequence of this behavior, the three structural modifications merge for the composition around $x = 0.12$ in BSnT [14] and a unique ferroelectric–paraelectric phase transition should take place at room temperature. Our data confirm such a behavior for the composition $x = 0.15$, which is the only one to have a superposition of crystalline symmetries (cubic and tetragonal) as demonstrated by the XRD analysis. This feature creates the possibility of reaching very high permittivities at room temperature for given compositions and makes these range of compositions very interesting for further investigations, both from applicative and from fundamental point of view [25].

Table 2 indicates the temperatures corresponding to the maximum permittivity, the Curie–Weiss temperatures T_0 and the maximum permittivity at 1 kHz for the present investigated BSnT compositions. With respect to BT, the maximum permittivity at the Curie temperature T_C initially increases for small Sn additions, reaches a maximum of ∼9000 for $x = 0.05$ at ∼90 °C and then decreases for concentrations higher than 0.10 (Table 1). In addition, the shape of the $\varepsilon(T)$ curves indicates that by increasing the Sn concentration, a relaxor behavior is progressively induced.

For $x = 0.15$ and $x = 0.20$, the relaxor character with diffuse phase transitions (DPT) and a frequency dispersion both for permittivity and tangent loss is observed, as shown in Fig. 5 for $x = 0.20$. For the full relaxor state, a Vogel–Fulcher frequency dependence of the maximum permittivity temperature with frequency was commonly reported in relaxors [26,27]. However, the very small frequency shift of T_m with frequency does not allow performing such a detailed analysis. In any case, it is clear that for high Sn additions ($x = 0.15$ and $x = 0.20$), the relaxor-paraelectric transition takes place in a large range of temperatures and not at a fixed Curie temperature T_C as for the compositions with $x = 0$ and 0.05. In this temperature range, the maximum permittivity temperature T_m is also located. The frequency dispersion observed for the tangent loss

Table 2
The critical temperatures and maximum values of permittivity for $BaSn_xTi_{1-x}O_3$ ceramics with various compositions.

Composition	$x=0$	$x=0.05$	$x=0.1$	$x=0.15$	$x=0.2$
Maximum permittivity temperature (T_C or T_m)	125 °C	90 °C	50 °C	16 °C	−20 °C
Curie–Weiss temperature from linear fits (T_0)	100 °C	83 °C	66.5 °C	38 °C	0 °C
Maximum value of permittivity ε_m	6916	9772	10,029	5824	3445

at high temperature in the paraelectric state (Fig. 5b) is not related to the relaxor behavior, but with thermally activated Maxwell Wagner relaxations, as commonly reported for solid solutions [28]. The dielectric data of our solid solutions are similar to ones reported in the literature for similar compositions [11,20].

A method to put in evidence the increasing relaxor character when increasing the Sn addition x is to use empirical formula derived from the Curie–Weiss law, as proposed in the Ref. [29] and often used for other $BaTiO_3$-based solid solutions like BZT [30,31] or for Pb-based relaxors [32]:

$$\varepsilon = \frac{\varepsilon_m}{1 + \left(\frac{T-T_m}{\delta}\right)^{\eta}} \quad (1)$$

This equation, with unique values of parameters η and δ for all the frequencies, describes the dielectric properties of relaxors, even in the dielectric dispersion region [33,34]. The parameter η gives information on the character of the phase transition: for $\eta=1$, normal Curie–Weiss law is obtained while $\eta=2$ describe a complete diffuse phase transition. In the latter case, δ has the dimension of a temperature and indicates the range of temperature extension for the diffuse phase transition, owing to the direct correlation with the dielectric permittivity broadening. For a ferroelectric material, Eq. (1) reduces to the Curie–Weiss law with $\eta=1$ and in this situation

Table 3
Computed empirical parameters η and δ by fits with Eq. (1) of the dielectric data of $BaSn_xTi_{1-x}O_3$ ceramics with various compositions at $f=1$ kHz.

Composition	$x=0$	$x=0.05$	$x=0.1$	$x=0.15$	$x=0.2$
η	1.01	1.17	1.65	1.68	1.72
$\ln\delta$	3.07	2.72	3.55	3.8	4.0
δ (°C)	21.5	15.2	34.8	44.7	54.6

δ is proportional to the Curie constant. Table 3 shows the values of these parameters for the studied compositions, as resulted from the linear fit of the dielectric data according to the Eq. (1). The evolution towards the relaxor state with increasing x is demonstrated by the increasing of both the empirical parameteres η (which increases from 1.03 at $x=0$ to 1.72 at $x=0.20$) and of the temperature extension of the diffuse phase transition δ (which increases from 16.4 at $x=0.05$ to 54.6 at $x=0.20$).

Further, an investigation of the frequency influence on the dielectric properties for these compositions was performed in the frequency range of 1–10^6 Hz. The frequency dependence of the real and imaginary part of permittivity at room temperature is shown in Fig. 6(a) and (b), respectively. Besides a monotonous reduction of

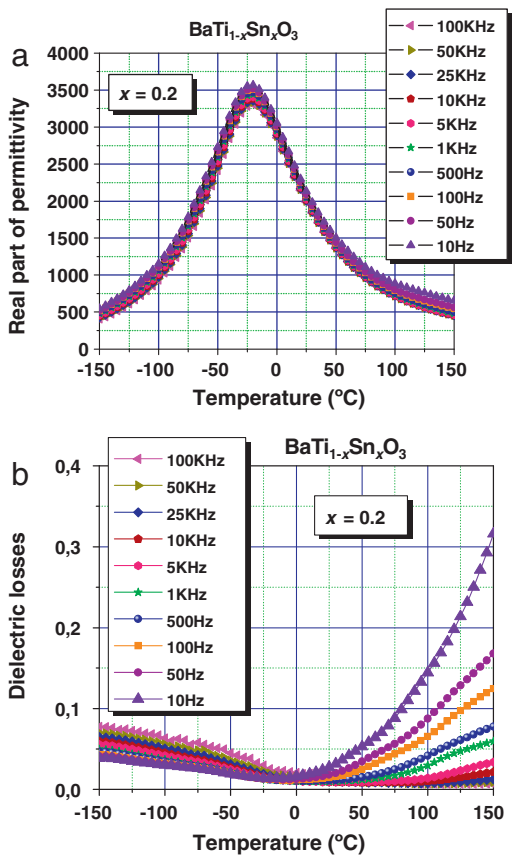

Fig. 5. Temperature dependence of the real part of the dielectric constant (a) and tangent loss tan δ (b) for $BaSn_xTi_{1-x}O_3$ with Sn content $x=0.2$ at different frequencies.

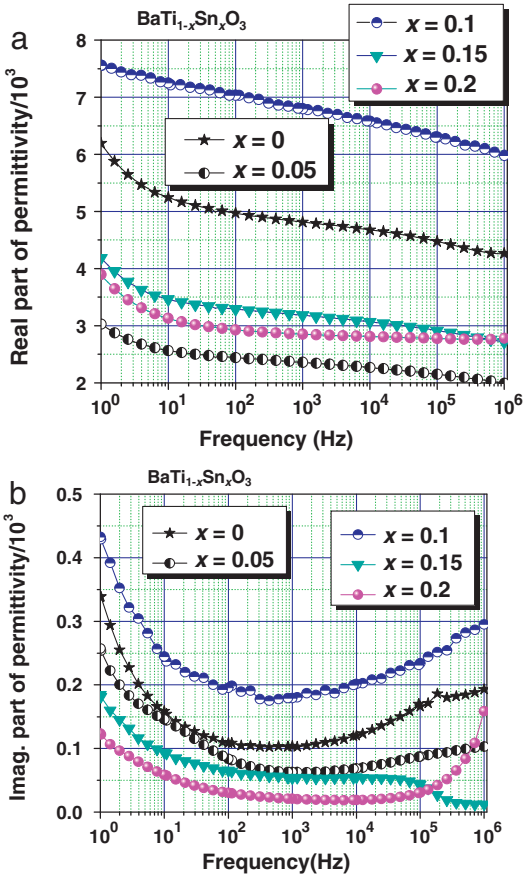

Fig. 6. Frequency dependence of the: (a) real part, (b) imaginary part of the dielectric constant of $BaSn_xTi_{1-x}O_3$ with various compositions x, at room temperature.

real part of permittivity with frequency, a few characteristic relaxations appear in specific frequency ranges, characterized by typical dielectric relaxation phenomena:

(i) The increasing of the real and imaginary parts of permittivity at low frequencies below 1 Hz for all the compositions is most probably associated to the thermally activated space charge effects at low frequencies (Maxwell–Wagner phenomena), possible related to the presence of oxygen vacancies in the sintered ceramics or to small grain boundary electrical inhomogeneities [28];

(ii) Small frequency dispersion visible in the real part of permittivity (Fig. 6a) in the range of 10–10^4 Hz for the large majority of compositions, with exception of the relaxor $x = 0.2$, which at room temperature is far to its Curie range. Similar relaxations were reported in the Ref. [35] and it was explained in terms of a non-Debye polar polydispersive relaxation;

(iii) Anomalies of the imaginary part of permittivity above 10^4 Hz for all the compositions (Fig. 6b), which seems to be related to a Debye-type relaxation process with characteristic frequencies in the range of 10^6–10^7 Hz, whose distribution of relaxation times strongly increases with Sn addition and tends to a glassy state for $x \geq 0.20$, due to the freezing of the nanopolar regions [37];

(iv) At high frequencies (not shown in the Figure), the permittivity tend to stabilize to composition dependent intrinsic values of: ~5980 ($x = 0.15$), ~5135 ($x = 0.10$), ~2980 ($x = 0$), ~2350 ($x = 0.20$) and ~1890 ($x = 0.05$), for 10^7 Hz.

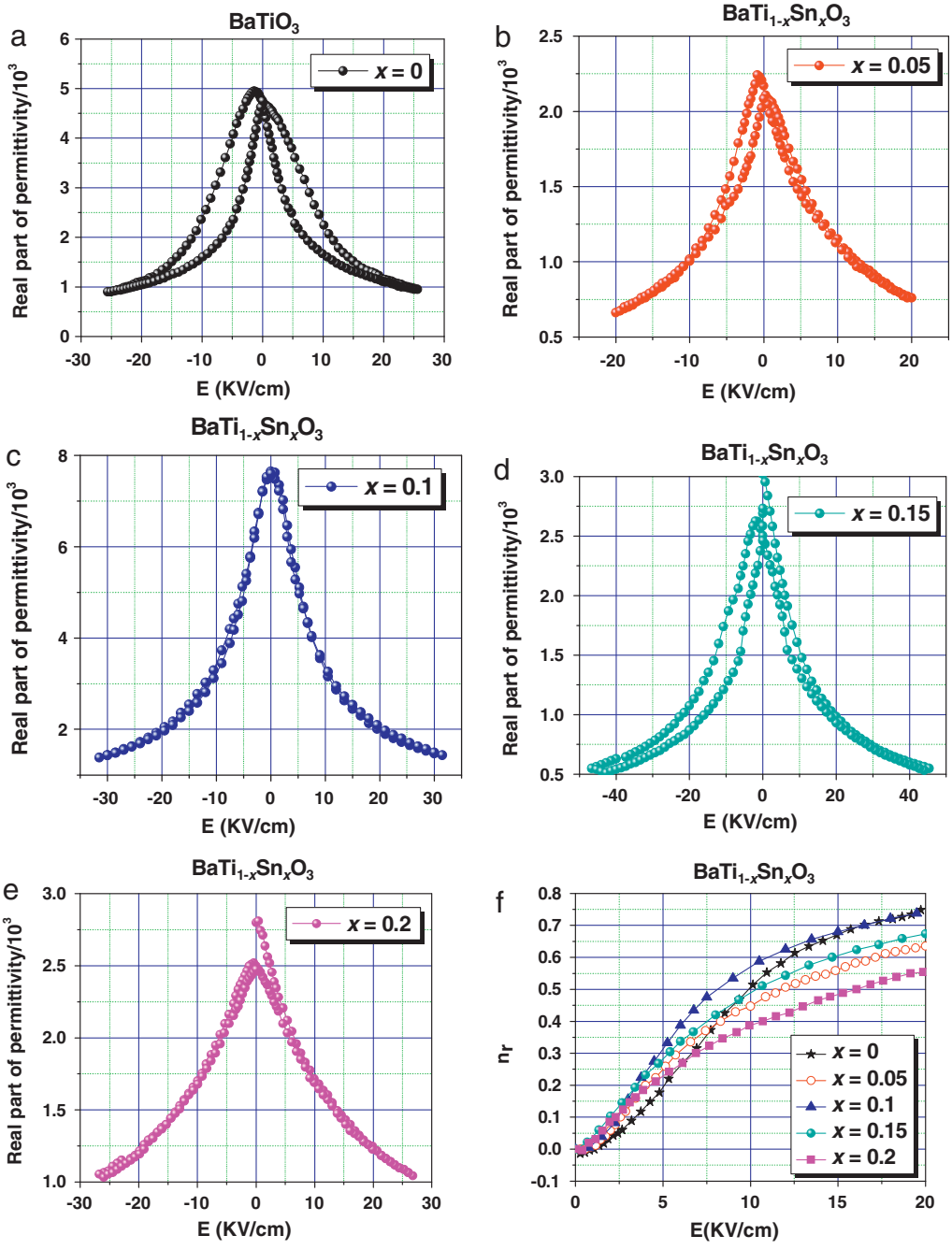

Fig. 7. Field dependence of the dielectric constant of $BaSn_xTi_{1-x}O_3$ ceramics at room temperature, at increasing/decreasing field, for various compositions: (a) $x = 0$, (b) $x = 0.05$, (c) $x = 0.10$, (d) $x = 0.15$, (e) $x = 0.20$ and (f) relative tunability for all the compositions.

The dielectric relaxations of the present ceramics are rather complex phenomena, due to the overlapped multiple contributions from: (a) the ferroelectric-relaxor crossover and its associated dipolar relaxation mechanisms which are expected to modify when increasing Sn addition (b) the charged defect-related relaxations caused by the oxygen vacancies present in the perovskite solid solutions which might be different in various ceramic samples [36] (c) grain core-grain boundary inhomogeneities of the electrical properties (grain boundary phenomena) [37,38] and other possible effects, imposing a more detailed study which is beyond of the purpose of the present work.

The compositions $x = 0.10$ and $x = 0.15$ have the highest intrinsic permittivity values at room temperature, due to the proximity of their ferroelectric–paraelectric phase transition and to the possible existence of mixed phases. As observed from Fig. 6, the best dielectric properties in a large range of radiofrequencies (below 10^2 kHz), with highest permittivity and lowest losses is showed at room temperature by the composition $x = 0.10$.

3.3. DC-tunability

The $\varepsilon(E)$ dependences (dc-tunability) of the BSnT ceramics were determined at room temperature at increasing/decreasing dc-field and they are shown in Fig. 7. A strong nonlinearity is observed for all the compositions, with a tendency towards saturation for high fields (~20 kV/cm). After the first increasing/decreasing cycles of the dc-field, the non-linear field-dependence $\varepsilon(E)$ tends to stabilize and the tunability data are reproducible. All the ceramics show a relative tunability, $n_r = (\varepsilon(0) - \varepsilon(E))/\varepsilon(0)$ in the range between 0.55 for $x = 0.2$ and 0.74 for $x = 0.1$, for a given value of the applied field of ($E = 20$ kV/cm). The dielectric losses remain below 10% at any field for all the investigated compositions.

Similar values of tunability were reported for $x = 0.10$ [18] and for $x = 0.2$ [39], but in addition, they were accompanied by clockwise ferroelectric $P(E)$ loops and abnormal domain switching mechanisms.

As expected, the hysteretic nature of the $\varepsilon(E)$ curve tends to reduce when the Sn addition increases, together with the ferroelectric-relaxor crossover. Such a behavior is observed for all the compositions, with the exception of $x = 0.15$, for which a hysteretic $\varepsilon(E)$ curve is again observed. In addition, its $\varepsilon(E)$ dependence seems to present a non-uniform decrease with the increasing field, like being resulted from components with different high-field behaviors. The observed feature most probably corresponds to the presence of the mixture of phases (cubic and tetragonal), as resulted from the XRD data. The nonlinear properties of these solid solutions should be further analyzed in detail, at various fields and temperatures, as well as from the point of view of their field stability, in order to understand features related to the crystalline phases and their superposition.

4. Conclusions

Pure perovskite $BaSn_xTi_{1-x}O_3$ ceramics with different tin contents ($x = 0$; 0.05; 0.1; 0.15 and 0.2) were prepared by a solid state reaction method. The XRD analysis shows a tendency of transition from tetragonal to cubic when increasing the Sn addition, with a superposition of both cubic and tetragonal symmetries for the composition $x = 0.15$. The dielectric data indicate a reducing of the Curie temperature with increasing of Sn content and a ferroelectric-relaxor crossover. The relaxor state became predominant for the compositions $x = 0.15$ and $x = 0.2$. The non-linear dielectric properties (tunability) of the ceramic samples at room temperature were studied in detail. When increasing the Sn addition, the $\varepsilon(E)$ dependence tends to reduce its hysteresis, while transforming into a non-hysteretic relaxor. Exceptionally, the composition $x = 0.15$ shows again a hysteretic $\varepsilon(E)$ feature, which was described as being derived from its composed tetragonal–cubic structure. The optimum tunable properties were found for the composition $x = 0.10$ (the highest relative tunability of 0.74 at the applied field $E = 20$ kV/cm and dielectric losses below 10%). Further, a detailed study related to the local crystalline symmetry, possible superposition of phases and Sn/Ti local inhomogeneities in relationship with the preparation method, purity and microstructures will be performed, for a better understanding of their role on the functional properties of the $BaSn_xTi_{1-x}O_3$ system.

Acknowledgments

The first author acknowledges the support of ESF-POSDRU 88/1.5/S/47646 (2007-2013) grant and S.Tascu the CNCSIS-PN-II-RU-RP nr. 2/03.11.2008 project.

References

[1] L. Mitoseriu, V. Tura, C. Papusoi, T. Osaka, M. Okuyama, Ferroelectrics 223 (1999) 99–106.
[2] Z. Yu, C. Ang, R. Guo, A.S. Bhalla, J. Appl. Phys. 92 (2002) 2655–2657.
[3] W.H. Payne, V.J. Tennery, J. Am. Ceram. Soc. 48 (1965) 413–417.
[4] A. Chen, Y. Zhi, J. Zhi, Phys. Rev. B 61 (2000) 957–961.
[5] J. Zhi, A. Chen, Y. Zhi, P.M. Vilarinho, J.L. Baptista, J. Appl. Phys. 84 (1998) 983–986.
[6] X. Wei, Y.J. Feng, X. Yao, Appl. Phys. Lett. 83 (2003) 2031–2033.
[7] G.A. Smolensky, J. Phys. Soc. Jpn. 28 (1970) 26–37.
[8] S.G. Lu, Z.K. Xu, H. Chena, Appl. Phys. Lett. 85 (2004) 5319–5321.
[9] A.K. Tagantsev, V.O. Sherman, K.F. Astafiev, J. Venkatesh, N. Setter, J. Electroceram. 11 (2003) 5–66.
[10] X. Wei, Y. Feng, X. Yao, Appl. Phys. Lett. 84 (2004) 1534–1536.
[11] X. Wei, Y. Feng, X. Yao, Appl. Phys. Lett. 83 (2003) 2031–2033.
[12] V. Mueller, H. Beige, Appl. Phys. Lett. 84 (2004) 1341–1343.
[13] V. Mueller, L. Jäger, H. Beige, H-P. Abicht, Th. Müller, Solid State Commun. 129 (2004) 757–760.
[14] X. Wei, X. Yao, Mat. Sci. Eng. B 137 (1–3) (2007) 184–188.
[15] V.V. Shvartsman, J. Dec, Z.K. Xu, J. Banys, P. Keburis, W. Kleemann, Phase Transit. 81 (2008) 1013–1021.
[16] L. Geske, V. Lorenz, T. Muller, L. Jager, H. Beige, H.P. Abicht, V. Mueller, J. Eur. Ceram. Soc. 25 (2005) 2537–2542.
[17] L. Geske, V. Muller, H. Beige, Ferroelectrics 361 (2007) 37–44.
[18] X. Wei, Y. Feng, L. Hang, S. Xia, L. Jin, X. Yao, Mater. Sci. Eng. B 120 (2005) 64–67.
[19] X. Wei, Y. Feng, X. Wan, X. Yao, Ceram. Int. 30 (2004) 1397–1400.
[20] W. Cai, Y. Fan, J. Gao, J. Mater. Sci.: Mater. Electron. (2010), doi:10.1007/s10854-010r-r0126-7.
[21] S. Markovic, M. Mitric, N. Cvjeticanin, D. Uskokovic, J. Eur. Ceram. Soc. 27 (2007) 505–509.
[22] F.M. Tufescu, L. Curecheriu, A. Ianculescu, C.E. Ciomaga, L. Mitoseriu, J. Optoelectron. Adv. Mater. 10 (2008) 1894–1897.
[23] V. Mueller, H. Beige, H.P. Abicht, C. Eisenschmidt, J. Mater. Res. 19 (2004) 2834–2840.
[24] C. Lei, A.A. Bokov, Z.G. Ye, J. Appl. Phys. 101 (2007) 084105-1–084105-9.
[25] Z. Yu, R. Guo, A.S. Bhalla, J. Appl. Phys. 88 (2000) 410–415.
[26] Z.G. Ye, Key Eng. Mater. 155–156 (1998) 81–122.
[27] R. Pirc, R. Blinc, Phys. Rev. B 76 (2007) 020101(R).
[28] I. Rivera, A. Kumar, N. Ortega, R.S. Katiyar, S. Lushnikov, Solid State Commun. 149 (2009) 172–176.
[29] I.A. Santos, J.A. Eiras, J. Phys. Condens. Matter 13 (2001) 11733–11740.
[30] C. Ciomaga, M. Viviani, M.T. Buscaglia, V. Buscaglia, L. Mitoseriu, A. Stancu, P. Nanni, J. Eur. Ceram. Soc. 27 (2007) 4061–4064.
[31] D. Ricinschi, C.E. Ciomaga, L. Mitoseriu, V. Buscaglia, M. Okuyama, J. Eur. Ceram. Soc. 30 (2010) 237–241.
[32] L. Mitoseriu, A. Stancu, C. Fedor, P.M. Vilarinho, J. Appl. Phys. 94 (2003) 1918–1925.
[33] A.K. Tagantsev, J. Lu, S. Stemmer, Appl. Phys. Lett. 86 (2005) 032901-1–032901-3.
[34] U. Bianchi, J. Dec, W. Kleemann, J.G. Bednorz, Phys. Rev. B 51 (1995) 8737–8746.
[35] V.V. Shvartsman, W. Kleemann, J. Dec, Z.K. Xu, S.G. Lu, J. Appl. Phys. 99 (2006) 124111-1–124111-3.
[36] X. Wei, X. Wan, X. Yao, J. Electroceram. 21 (2008) 226–229.
[37] H. Beltrán, E. Cordoncillo, P. Escribano, D.C. Sinclair, A.R. West, J. Appl. Phys. 98 (2005) 094102-1–094102-7.
[38] N. Masó, M. Prades, H. Beltrán, E. Cordoncillo, D.C. Sinclair, A.R. West, Appl. Phys. Lett. 97 (2010) 062907-1–062907-3.
[39] T. Wang, X.M. Chen, X.H. Zheng, J. Electroceram. 11 (2003) 173–178.